Research Article

Journal of MASS SPECTROMETRY

Received: 7 May 2008 Accepted: 29 August 2008 Published online in Wiley Interscience: 17 November 2008

(www.interscience.com) DOI 10.1002/jms.1508

Online H/D exchange liquid chromatography as a support for the mass spectrometric identification of the oxidation products of melatonin

Fabrice Collin,[a]* Dominique Bonnefont-Rousselot,[b,c] Saïd Yous,[d] Catherine Marchetti,[a] Daniel Jore[a] and Monique Gardès-Albert[a]

The hydrogen–deuterium exchange of protonated melatonin and its *in vitro* oxidation end-products have been examined by liquid chromatography coupled with ion-trap mass spectrometry. Specific H/D scrambling of protons in the C2 and C4 positions of the indole ring during gas-phase fragmentation process was observed for both melatonin and its oxidation products. Collision-induced dissociation spectra showed losses of variably deuterated NH_3, H_2O and CH_3CONH_2. In addition, a similar H/D scrambling behaviour was observed for the oxidation products, obtained from the opening of the indole ring by oxidative attack. Fragmentation pathways are proposed and H/D scrambling has been employed as a fingerprint, allowing identification of N^1-acetyl-5-methoxykynurenin (AMK), N^1-acetyl-N^2-formyl-5-methoxykynurenin (AFMK), dehydro-AFMK and hydroxymelatonin as the oxidation products of melatonin *in vitro*. Copyright © 2008 John Wiley & Sons, Ltd.

Keywords: melatonin; hydroxyl radicals; deuterium exchange; liquid chromatography; mass spectrometry; oxidation

Introduction

Melatonin (MLT) or *N*-acetyl-5-methoxytryptamine is a pineal hormone whose direct and indirect antioxidant properties have been recognised.[1,2] Apart from its effects on the circadian rhythm, antioxidant properties have been reported both *in vitro*[3,4] and *in vivo*[5–7] regarding the lipid peroxidation and DNA degradation. The latter action could be related to a direct scavenging of free radicals and/or an activation of DNA repair enzymes.[8] Several studies have demonstrated the ability of MLT to scavenge the oxygen-derived free radicals, such as hydroxyl[9–11] and peroxyl[12,13] radicals, although it does not seem to react with superoxide radicals.[14,15] Moreover, the protective effects of MLT have been reported for *in vitro* oxidation of low-density lipoproteins (LDL) by copper or by macrophages.[12,14,16,17] This protection has been explained by the ability of MLT to directly scavenge the lipid-free radicals involved in these oxidation processes.[18] Similarly, the models of MLT-loaded nanoparticles have shown their efficiency in protecting liposomes or microsomes against lipid peroxidation.[19]

Although some metabolites have been identified *in vivo*,[20] the mechanisms by which MLT displays its antioxidant properties have not totally been elucidated. To improve the knowledge of the MLT antioxidant mode of action, this work has focused on the direct antioxidant properties of MLT *in vitro* against hydroxyl free radicals generated in aerated aqueous solution by gamma radiolysis. Gamma radiolysis of water is a powerful method that allows a homogeneous production of known quantities of free radical species, since radiolytic yields (number of free radicals produced per unit energy absorbed) are well known for each species.[21] Free radicals thus generated, particularly hydroxyl radical, were used to initiate one-electron oxidation of MLT dissolved in water. This study was designed to characterise the oxidation end-products of MLT by mass spectrometry and, in particular, by using the specific H/D exchange behaviour of MLT as a tool for identification of the fragmentation pathways.

Experimental

Reagents

MLT was obtained from Sigma (reference M5250, Saint-Quentin Fallavier, France). Stock aqueous solutions of MLT (10^{-3} mol l^{-1} and 5×10^{-4} mol l^{-1}) were prepared directly by dissolving the powder in ultra-pure water (Maxima Ultra-pure water, ELGA, resistivity: 18.2 MΩ), using a magnetic stirrer for 30 min at room temperature. Aqueous solutions of MLT are stable for at least

* *Correspondence to: Fabrice Collin, Laboratoire de Chimie Physique, CNRS UMR 8601, Université Paris Descartes, 45 rue des Saints Pères, 75006 Paris, France. E-mail: fabrice.collin@univ-paris5.fr*

a *Laboratoire de Chimie-Physique, CNRS UMR 8601, Université Paris Descartes, 45 rue des Saints-Pères, 75006 Paris, France*

b *Laboratoire de Biochimie Métabolique et Clinique (EA 3617), Université Paris Descartes, 4 avenue de l'Observatoire, 75006 Paris, France*

c *UF de Biochimie des Maladies Métaboliques, Service de Biochimie Métabolique, Bâtiment Benjamin Delessert, Hôpital de La Pitié (AP-HP), 83 boulevard de l'Hôpital, 75013 Paris, France*

d *Institut de Chimie Pharmaceutique, Université de Lille 2, Rue du Professeur Laguesse, BP 83, 59006 Lille, France*

Journal of MASS SPECTROMETRY

15 days, displaying no chemical modifications, as checked by UV-visible spectrophotometry. MLT has a pK_a of 12.3[22] that implies one deprotonation of the nitrogen of the pyrrole ring (NH/N^- acid-base couple), so that at pH 7 MLT is preferentially in the protonated form (Fig. 1). Irradiations were carried out in test tubes that had been previously cleaned with hot TFD4 detergent (Franklab S.A., France), rinsed thoroughly with ultra-pure water, and then heated to 400 °C for 4 h to avoid any contamination by remaining organic compounds.

Generation of reactive oxygen species by water radiolysis

Radiolysis corresponds to the chemical transformations of a solvent because of the absorption of ionising radiation, which produces a homogeneous solution of free radicals within a few nanoseconds. Radiolytically generated free radicals are independent of the nature and concentration of the dissolved compound as long as its concentration remains lower than or equal to 10^{-2} mol l^{-1}.[21]

Gamma radiolysis was carried out using an IBL 637 irradiator (CIS Biointernational, Gif-sur-Yvette, France), a ^{137}Cs source, whose activity was approximately 222 TBq (6000 Ci). A dose rate of 9.76 Gy/min was used. The dosimetry was determined by the Fricke method,[21,23] namely radiooxidation of 10^{-3} mol l^{-1} ferrous sulfate solution in 0.4 mol l^{-1} sulfuric acid (under an aerated atmosphere) taking λ_{max} (Fe^{3+}) = 304 nm, $\varepsilon_{(304\ nm)}$ = 2204 l mol^{-1} cm^{-1} at 25 °C and a radiolytic yield of G(Fe^{3+}) = 1.62 μmol J^{-1}. Different radiation doses, ranging from 10 to 440 Gy, were delivered to 5 ml of the aqueous solution of MLT, depending on the duration of exposure to the γ-ray source: the longer the time, the higher the radiation dose. For each experimental set, 5 ml of non-irradiated solution was used as a control.

Water radiolysis by γ-rays generates the free radical species e^-_{aq}, •OH, •H and the molecular species H_2 and H_2O_2. Under aerated conditions (oxygen concentration approximately 2×10^{-4} mol l^{-1}), hydroxyl and superoxide radicals (resulting from the scavenging of e^-_{aq} and •H species) were simultaneously produced with the radiolytic yields (G-values expressed in moles per Joule) of 2.8×10^{-7} and 3.4×10^{-7} mol J^{-1}, respectively. In this study, only hydroxyl radicals were considered as a potent oxidant of MLT, because superoxide radicals are not able to initiate the oxidation of MLT.[14,15]

Analysis

Analyses were performed on an ion-trap mass spectrometer (LCQ Advantage, Thermofinnigan, Les Ulis, France) equipped with an electrospray ionisation (ESI) source. The capillary temperature was held at 250 °C and the relative sheath and auxiliary gas flow-rates were set at 20 and 5, respectively (sheath gas, 0–100 units corresponding to 0–1.5 l min^{-1}, auxiliary gas, 0–60 units corresponding to 0–18 l min^{-1}, according to the manufacturer's specifications). Other parameters, such as lens or capillary voltages, were tuned systematically to obtain the best signal intensities for each ion of interest. All experiments were performed in the positive-ion mode, and each spectrum was typically an average of 20 scans. MS/MS and MS^3 experiments were performed on mass-selected ions in the ion-trap mass spectrometer using standard isolation and excitation procedures.

For direct infusion analysis, irradiated MLT samples were diluted 10:1 (v/v) with methanol prior to being infused continuously into the ESI source with an SGE 250 μl syringe at a flow-rate of 12.5 μl min^{-1}. To study deuterium exchange on MLT and its oxidation end-products, 5 ml of irradiated and non-irradiated MLT aqueous solutions was lyophilised to dryness and rediluted into the labelled medium D_2O/MeOD (1/1 v/v). Deuterium oxide and deuterated methanol have minimum isotopic purities of 99.96 and 99.5% D, respectively, and were from Aldrich Chemicals (Milwaukee, WI, USA).

In addition, high-performance liquid chromatographic/mass spectrometric (HPLC/MS) experiments were conducted (Surveyor, Thermoquest, Les Ulis, France) by eluting with either non-deuterated or deuterated solvents. As much as 5 ml of irradiated and non-irradiated MLT aqueous solutions was lyophilised to dryness and rediluted into 500 μl of H_2O or D_2O. Chromatographic conditions were as follows: 20 μl of sample was injected onto the column (Kromasil C18 250 × 2.1 mm, 5 μm, Ait-Chromato, France), whose temperature was held at 40 °C. The elution was achieved with a mobile phase consisting of a mixture H_2O/acetonitrile or D_2O/acetonitrile (80/20, v/v) and delivered at a flow-rate of 250 μl min^{-1}. The mass spectrometer was used as a detector, working in the full-scan mode between 100 and 400 Da and in the dependent scan mode, allowing the fragmentation of selected precursor ions (typical isolation width of 1 Da and collision energy set at 34%: units as given by the manufacturer).

Results and Discussion

Deuterium exchange and fragmentation pathway of non-oxidised MLT

A collision-induced dissociation (CID) spectrum was obtained for a solution of MLT (100 μmol l^{-1}) in H_2O/MeOH (1/10 v/v) and is presented in Fig. 1. The precursor ion is detected at *m/z* 233.1 and main fragments at *m/z* 216.1, 191.0 and 174.1 corresponding to losses of 17, 42 and 59 Da, respectively. Initially, these losses could come from the aliphatic part of MLT (*N*-acetyl group) and correspond to NH_3, CH_2CO and (NH_3 + CH_2CO or CH_3CONH_2), respectively. As shown in Fig. 1 (inset), the ion at *m/z* 174.1 is generated by fragmentation of *m/z* 216.1. However, this fragment is also known as a direct product ion of protonated MLT,[24,25] by a loss of CH_3CONH_2.

MLT has two potential H/D exchangeable hydrogens (plus one for protonation), one on the *N*-pyrrolic group and the other on the *N*-acetyl group. An increase of +3 Da is therefore expected and protonated MLT should be detected exclusively at *m/z* 236.0 in D_2O/MeOD. However, even for MLT in pure labelled medium, three peaks at *m/z* 234, 235 and 236 were detected and were fragmented (Fig. 2). Although only fully deuterated MLT (*m/z* 236) is of interest, the isotopic contribution of *m/z* 234 and 235 could affect the abundance of products ions from fragmentation of *m/z* 236. Since MLT only contains 13 carbons, this isotopic contribution should be only due to *m/z* 235 and should not exceed approximately 13% (the contribution at M+2 from *m/z* 234 due either to one ^{18}O or two ^{13}C could be considered as negligible). Thus, the CID spectrum of *m/z* 236 is mainly a representative of the fragmentation of fully deuterated MLT and the isotopic contribution of *m/z* 235 should be considered as negligible regarding the abundances of fragmentation products of *m/z* 236.

Surprisingly, except for *m/z* 194.0, the fragmentation of the unique ion at *m/z* 236 (Fig. 2(c)) leads to multiple fragments at *m/z* 175.2, 176.2, 177.2 and *m/z* 217.1, 218.1 and 219.1. This suggests that H/D scrambling could occur during the gas-phase

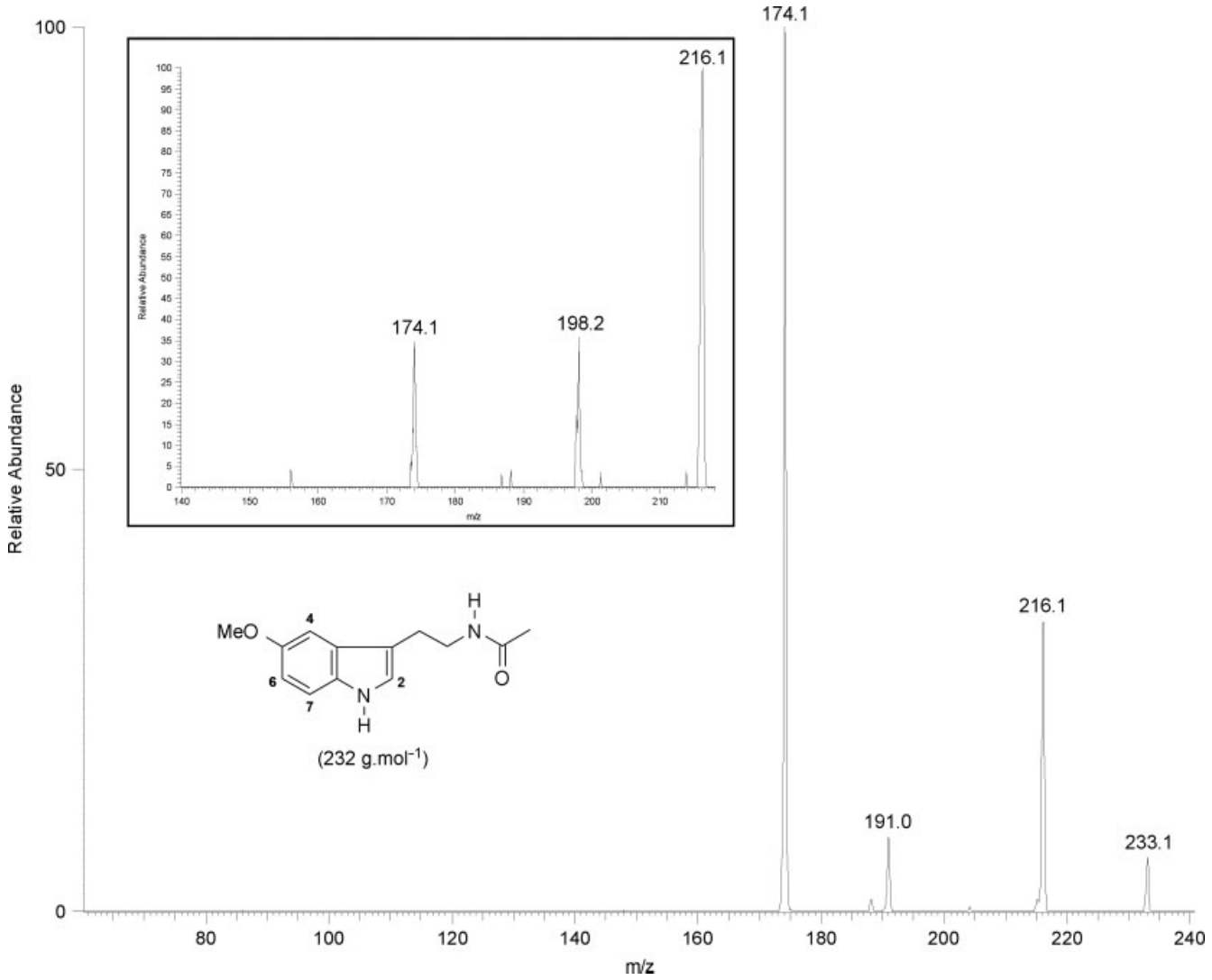

Figure 1. CID spectrum of the ion at *m/z* 233.1 for a non-irradiated solution of MLT (100 µmol l^{-1}). Inset: MS^3 spectrum of product ion at *m/z* 216.1.

fragmentation process, leading to variable losses and thus to a series of fragments that differ by 1 Da. In a previous study on deuterium exchange and fragmentation pathways of protonated tryptophan, Lioe *et al.*[26] demonstrated that two hydrogens located in the C2 and C4 positions of the pyrrole ring may exchange with the deuteriums of the terminal amine group. This leads to variable losses during the fragmentation of the aliphatic amino-acid group of tryptophan and is characterised by multiple peaks in CID spectra of deuterated tryptophan.

Since MLT is a tryptophan-like compound, H/D scrambling could occur during MLT fragmentation. Although the similarity between MLT and tryptophan is not an unequivocal proof, it is strong enough to argue for similar H/D scrambling, regarding the experimental evidences. Scheme 1 combines the proposed H/D scrambling and fragmentation pathways of MLT in D_2O/MeOD (even if deuteration is not needed to establish this latter). For MLT in D_2O/MeOD, *N*-pyrrolic and *N*-acetyl groups are deuterated: the latter could exchange twice with protons of the pyrrole ring during the gas-phase fragmentation process. This mechanism is in agreement with our experimental results on MLT fragmentation (Fig. 2(c)). By the loss of CH_2CO, fragmentation of *m/z* 236 generates an ion that is not affected by H/D scrambling, since it does not involve the *N*-acetyl group, and which is detected at *m/z* 194. Direct loss of CH_3CONHD or CH_3CONH_2 from *m/z* 236, according to the proposed fragmentation pathway, leads to fragments detected at *m/z* 176 and 177. The loss of neutral ammonia implies a rearrangement as suggested in Scheme 1 (pathway a), leading to the product ions detected at *m/z* 217, 218 and 219 (loss of NHD_2, NH_2D and NH_3, respectively), which may lose fixed-mass CH_2CO to generate second-generation ions at *m/z* 175, 176 and 177, respectively. This mechanism, involving an H/D exchange pre-equilibrium, is consistent with the CID spectrum of monodeuterated MLT (Fig. 2(a)), where only two consecutive peaks are detected at *m/z* 174.2, 175.1 and *m/z* 216.1, 217.1, and with the CID spectrum of doubly deuterated MLT (Fig. 2(b)), where three consecutive peaks are detected at *m/z* 174.1, 175.1, 176.1 and *m/z* 216.1, 217.1, 218.1. Though the full-scan spectrum of MLT in the deuterated medium exhibits three peaks, we were interested only in the fully deuterated ion of MLT (*m/z* 236) and its oxidation products. When the fully deuterated MLT is isolated into the trap, there is no possibility for back-exchange since the trap is under vacuum, and thus, triplet ions obviously result from intramolecular rearrangement. In addition, the presence of a single peak in the CID spectra corresponding to the loss of CH_2CO (see

Journal of MASS SPECTROMETRY

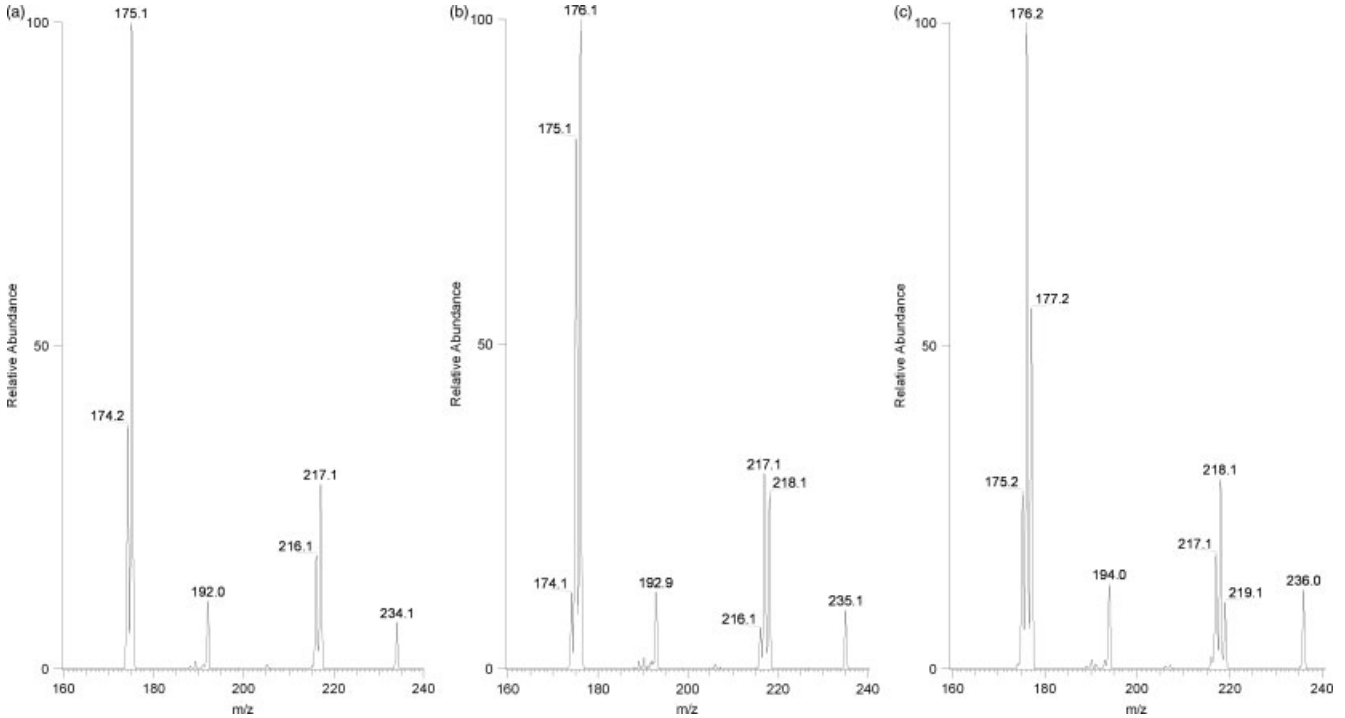

Figure 2. CID spectra of a solution of non-irradiated MLT (100 µmol l^{-1}) in D_2O/MeOD (1/1 v/v). (a) CID spectrum of the ion at *m/z* 234.1 (MLT + 1 exchange); (b) CID spectrum of the ion at *m/z* 235.1 (MLT + 2 exchanges); (c) CID spectrum of the ion at *m/z* 236.0 (MLT + 3 exchanges).

for example Scheme 1) is a proof that there is no deuterium loss during fragmentation. Otherwise, we would observe a multiple peak.

HPLC/MS study of oxidised MLT

During water radiolysis, molecular and radical oxygen species are generated continuously and homogeneously into the solution. Among them, the hydroxyl radical HO• is the most susceptible to react with MLT by abstracting a hydrogen atom, by abstracting an electron or by adding a double bond.[27] As MLT possesses several reaction sites for oxidation by HO• radicals, such as the indole ring, one pair of electrons of nitrogen atoms or the hydrogen on the aliphatic chain, the prediction of structures for oxidation products is difficult. Aerated aqueous solutions of MLT (100 µmol l^{-1}), non-irradiated (control) and irradiated at 300 Gy, were analysed by HPLC/MS and the results compared (Fig. 3). Protonated MLT (*m/z* 233.1) is detected at $t_r = 12.88$ min along with oxidation products that are absent from the control: *m/z* 237.1 at $t_r = 7.82$, *m/z* 249.1 at $t_r = 4.78$ and $t_r = 5.32$, *m/z* 263.1 at $t_r = 4.53$, and *m/z* 265.1 at $t_r = 6.96$.

Table 1 summarises the results obtained and, based on the mass difference observed with MLT, suggests structures for the oxidation products. Products at *m/z* 249 and 265 result from an addition of +16 and +32 Da, respectively, in comparison with *m/z* 233 (protonated MLT). As MLT is a target for reactive oxygen species, these differences could correspond to the addition of one or two atoms of oxygen, leading to the generation of hydroxyl or peroxide groups. The difference of +4 Da between *m/z* 237 and *m/z* 233 is more unusual, and structure prediction more difficult. However, some minor MLT metabolites have been identified *in vivo*,[28–30] including N^1-acetyl-5-methoxykynurenin (AMK) and N^1-acetyl-N^2-formyl-5-methoxykynurenin (AFMK) whose molecular weights (respectively 236 and 264 g mol^{-1}) could match our experimental results. The last oxidation product, detected at *m/z* 263, could be produced by dehydrogenation (e.g. generation of a double bond) of AFMK.

Identification of the product detected at *m/z* 237

The chemical structure of the oxidation product detected at *m/z* 237 is difficult to predict from the oxidation of MLT since the mass difference of +4 Da is unusual. Nevertheless, as mentioned above, AMK could be a good candidate since it has a molecular weight of 236 g mol^{-1} and could correspond to the product at *m/z* 237, which is generated by the oxidation of MLT *in vitro*.

To test this assumption, AMK was synthesised and analysed by mass spectrometry. Figure 4 shows CID spectra of synthetic AMK in D_2O/MeOD (Fig. 4(a)) and in H_2O/MeOH (Fig. 4(a), inset). The fragmentation of *m/z* 237.0 leads to four product ions at *m/z* 219.7, *m/z* 178.0, *m/z* 124.1 and *m/z* 114.0 (Fig. 4(a), inset). The MS^3 spectrum of the fragment at *m/z* 178.0 reveals no peak at *m/z* 114.0 or *m/z* 124.1 (data not shown).

Since it possesses three exchangeable hydrogens, fully deuterated AMK is detected at *m/z* 241.0 ($[AMK + D]^+$, Fig. 4(a)). The CID spectrum of AMK shows fragment ions appearing as multiple ions separated by 1 Da in mass, mainly at *m/z* 115.0, 116.0, 117.0 and *m/z* 180.1, 181.0, 182.0 and *m/z* 126.1, 127.1, 128.1 with lower intensity. H/D exchange between *N*-acetyl deuterium and a proton of the benzene ring during the gas-phase fragmentation process could be involved as with MLT for protons of the indole ring. This has already been experimentally observed with neurotransmitters, such as DL-DOPA, which present similar chemical structures.[31] However, this specific H/D scrambling cannot explain the presence of three consecutive peaks in the CID spectrum (*m/z* 115.0, 116.0, 117.0). Indeed, only one hydrogen is available on the benzene ring

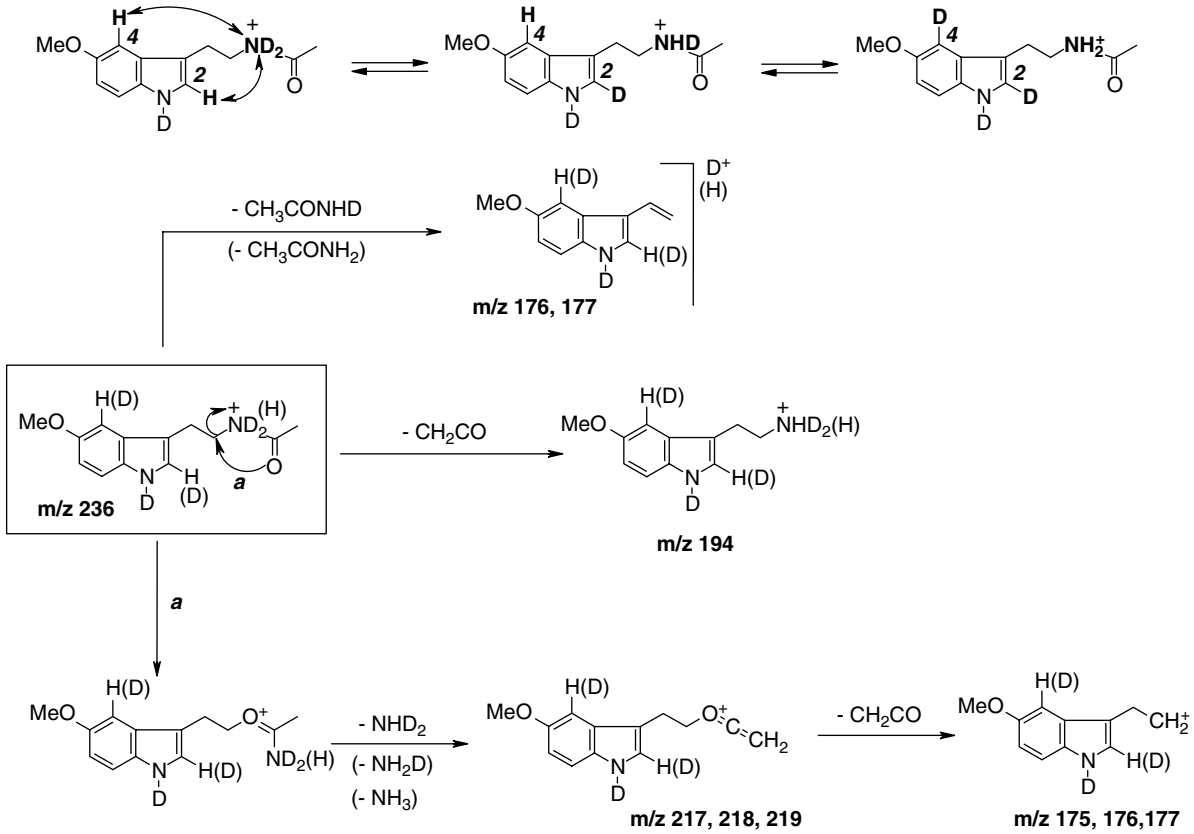

Scheme 1. The proposed H/D scrambling and fragmentation pathway for fully deuterated MLT (related to Fig. 2(c)).

Table 1. Oxidation products of melatonin (MLT) identified by HPLC/MS in aerated conditions (Fig. 3): based on the comparison of their masses with a reference parent mass, a possible identification is proposed

m/z	t_r (min)	Difference in mass/MLT[a]	Possible identification
237	7.82	[MLT + 1] + 4	AMK
249	4.78 5.32	[MLT + 1] + 16	Hydroxylated MLT(HO-MLT)
263	4.53	[MLT + 1] + 32−2	Dehydrogenated *m/z* 265
265	6.96	[MLT + 1] + 32	Doubly hydroxylated MLT or AFMK

[a] MLT: 232 g mol^{-1}, $[M + H]^+$ detected at *m/z* 233.1; AMK, N^1-acetyl-5-methoxykynurenin; AFMK, N^1-acetyl-N^2-formyl-5-methoxykynurenin.

for a single exchange. It can be assumed that another exchange could occur on the tautomeric form of AMK (Scheme 2): one deuterium of the amine group could exchange with one hydrogen of the enol group. Fragmentation of AMK at the bond between the benzene ring and the first carbonyl group thus leads to ions at *m/z* 126, 127, 128 and 115, 116, 117. Relative abundance (Fig. 4(a)) shows that charge is preferentially held by these last fragments. The second fragmentation pathway (Scheme 2) is similar to the one proposed for MLT (Scheme 1), with a loss of variably deuterated ammonia (NHD_2, NH_2D or NH_3) followed by the loss of CH_2CO, leading to three consecutive ions at *m/z* 222, 223, 224 and then *m/z* 180, 181, 182.

An aerated aqueous solution of MLT (100 µmol l^{-1}) was irradiated at 300 Gy, lyophilised to dryness, rediluted in D_2O and analysed by HPLC/MS in the dependent scan mode for comparison with the fragmentation pathway proposed for synthetic AMK. As expected, a chromatographic peak is detected at t_r = 10.89 min for *m/z* 241.1 (AMK + 4 deuterium exchanges) (Fig. 3). Figure 4(b) presents the corresponding CID spectrum, which resembles the CID spectrum of synthetic AMK: multiple fragment peaks are detected at corresponding *m/z* values, due to H/D scrambling occurring during the gas-phase fragmentation process. These observations suggest that AMK is an oxidation end-product of MLT *in vitro*.

Identification of the products detected at *m/z* 249

Two oxidation end-products of MLT are detected at *m/z* 249 (Table 1). The mass difference from MLT is +16 Da, suggesting the addition of one atomic oxygen in the form of a hydroxyl group, in agreement with the attack by hydroxyl free radicals during water radiolysis. Moreover, hydroxylation is one of the metabolic pathways of MLT *in vivo*. Several authors have reported that 6-hydroxymelatonin (6HO-MLT), 2-hydroxymelatonin (2HO-MLT)

Journal of MASS SPECTROMETRY

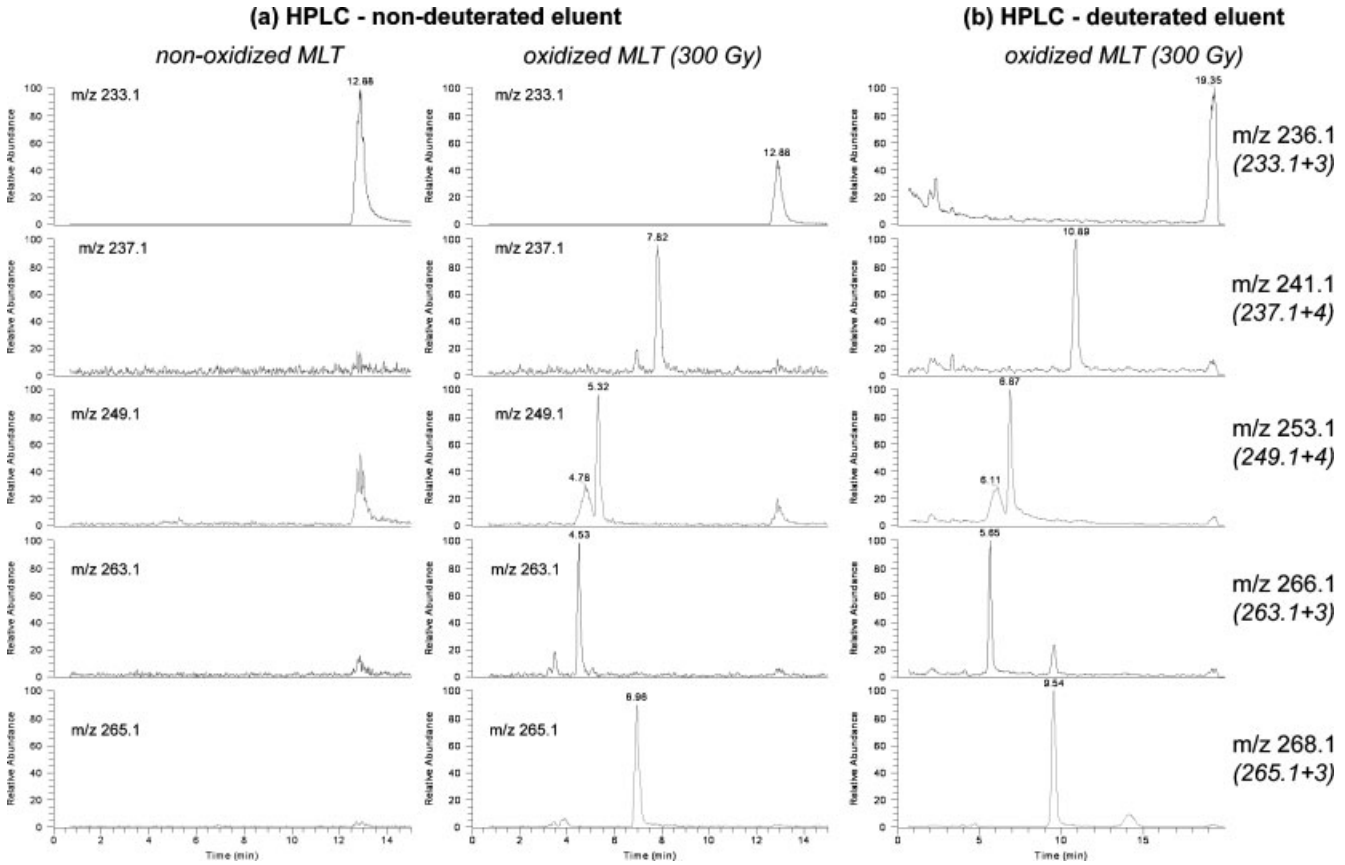

Figure 3. Trace chromatograms of MLT (*m/z* 233.1) and its oxidation products (*m/z* 237.1, 249.1, 263.1 and 265.1). (a) elution with H_2O/CH_3CN (80/20 v/v) and comparison between non-oxidised and oxidised MLT (300 Gy), (b) elution with D_2O/CH_3CN (80/20 v/v); under these operating conditions, masses under focus are incremented with the total number of possible deuterium exchanges for each product.

and cyclic 3-hydroxymelatonin (C3HO-MLT) are resultant products of MLT interaction with reactive oxygen species generated by Fenton-type reactions (see Ref. [32] for a review). Pulse radiolysis studies, closer to our experimental conditions (without the addition of metallic cations in solution), have shown that the C2, C3 and C7 positions of the indole ring are preferentially attacked by HO radicals.[11,22] A more recent paper reports a theoretical calculation of the $HO^{\bullet}$ radical reaction with MLT[33] and suggests that the C2 position is the most probable site of $HO^{\bullet}$ attack and the C3 position the least. However, because of the calculation method employed (AM1 semi-empirical Hamiltonian) and because the calculated activation barriers and reaction enthalpies values are very similar, uncertainty remains. All the HO-MLT products previously suggested being a result of an attack of hydroxyl radicals on the indole aromatic ring. Another possibility could be the hydroxylation of MLT on its aliphatic chain. The resulting product would be generated as following: abstraction of one hydrogen atom by $HO^{\bullet}$ on the aliphatic chain to make a carbon-centred radical, addition of molecular oxygen then biradicalar reaction to make a hydroperoxide, and finally, degradation of this latter to make a hydroxide species. If this product had been generated during the oxidation of MLT, the intermediate hydroperoxide would have been detected; it was not the case in our experimental conditions. Moreover, hydroxylation of MLT on its aliphatic chain has never been demonstrated in previous studies, *in vivo* or *in vitro*. One can assume that the rate constant of the addition of hydroxyl radical on the indole ring of MLT is much higher than the one of the abstraction of one hydrogen atom on the aliphatic chain.

The CID spectrum (direct infusion) of the ion detected at *m/z* 249.1 for an aerated aqueous solution of MLT (100 µmol l^{-1}) irradiated at 340 Gy is presented in Fig. 5(a), along with MS^3 spectra of product ions at *m/z* 231.1 (Fig. 5(b)) and *m/z* 207.1 (Fig. 5(c)). Fragmentation of the *m/z* 249.1 species leads to two product ions at *m/z* 231.1 and *m/z* 207.1 that are able to fragment again giving second-generation ions at *m/z* 189.0 and *m/z* 190.1, respectively. The main loss at −18 Da (*m/z* 249.1 → *m/z* 231.1) corresponds to water loss. Other losses are −42 Da (*m/z* 249.1 → *m/z* 207.1 and *m/z* 231.1 → *m/z* 189.1) and −17 Da (*m/z* 207.1 → *m/z* 190.1), also observed during MLT fragmentation (Fig. 1), and corresponding to CH_2CO and NH_3, respectively. The CID spectrum of the ion at *m/z* 249.1 seems to be in good agreement with the chemical structure of xHO-MLT.

As the chemical structures of xHO-MLT (Fig. 5(a)) and MLT are close, H/D scrambling of xHO-MLT is expected to be similar also. Figure 5(d) presents the CID spectra of the ion at *m/z* 252.1 for the chromatographic peak detected at $t_r = 6.11$ min (Fig. 5 (d1)) and of the ions at *m/z* 252.1 (Fig. 5 (d2)) and *m/z* 253.2 (Fig. 5 (d3)) for the chromatographic peak detected at $t_r = 6.87$ min. As expected, H/D scrambling is observed in every spectrum. A single peak at *m/z* 210.1 or *m/z* 211.1 is also detected. A similar fingerprint was observed for MLT (Fig. 2), with the presence of multiple peaks together with a single peak resulting from the loss of CH_2CO.

For the first product ($t_r = 6.11$ min, Fig. 5 (d1)), the particular transition *m/z* 252.1 → *m/z* 234.1 implies the loss of non-deuterated water (−18 Da), whereas *m/z* 252.1 → *m/z* 232.2 implies the loss of deuterium oxide (−20 Da), thus highlighting

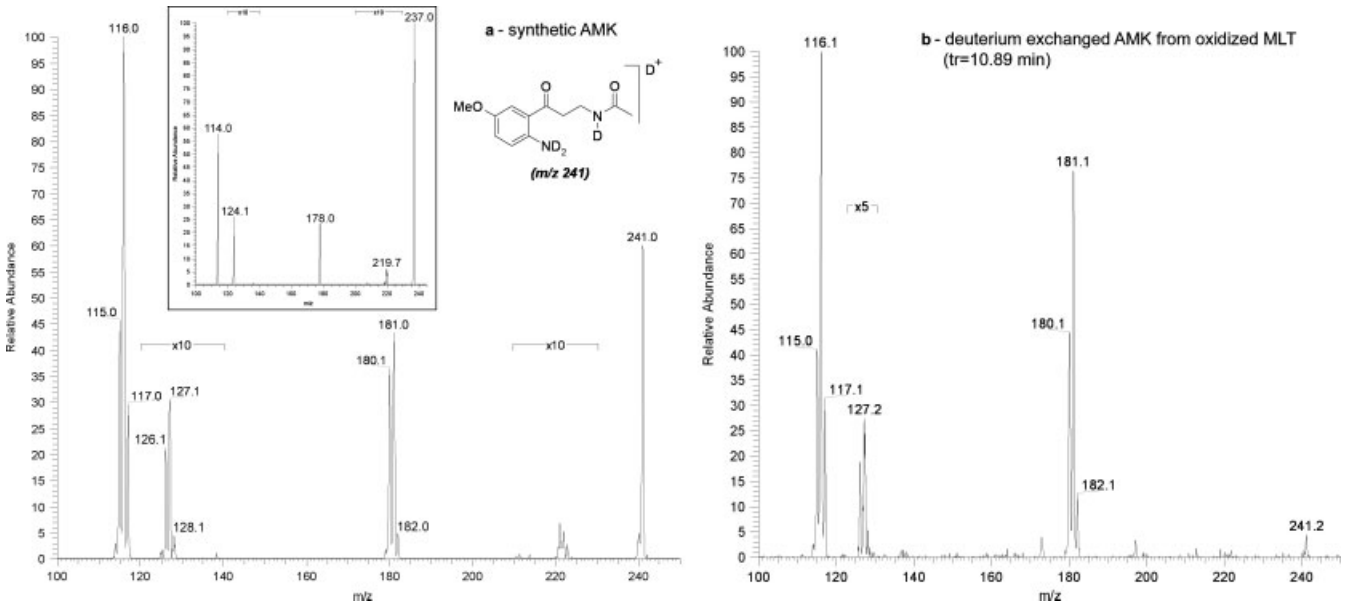

Figure 4. (a) CID spectrum of synthetic AMK (50 µmol l^{-1}), in D_2O/MeOD (1/1, v/v) and in H_2O/MeOH (inset), (b) CID spectrum of the ion at *m/z* 241.2 (*m/z* 237 + 4 deuterium exchanges) for the chromatographic peak detected at t_r = 10.89 min: retention time refers to the chromatogram obtained for HPLC working with deuterated eluent (Fig. 3).

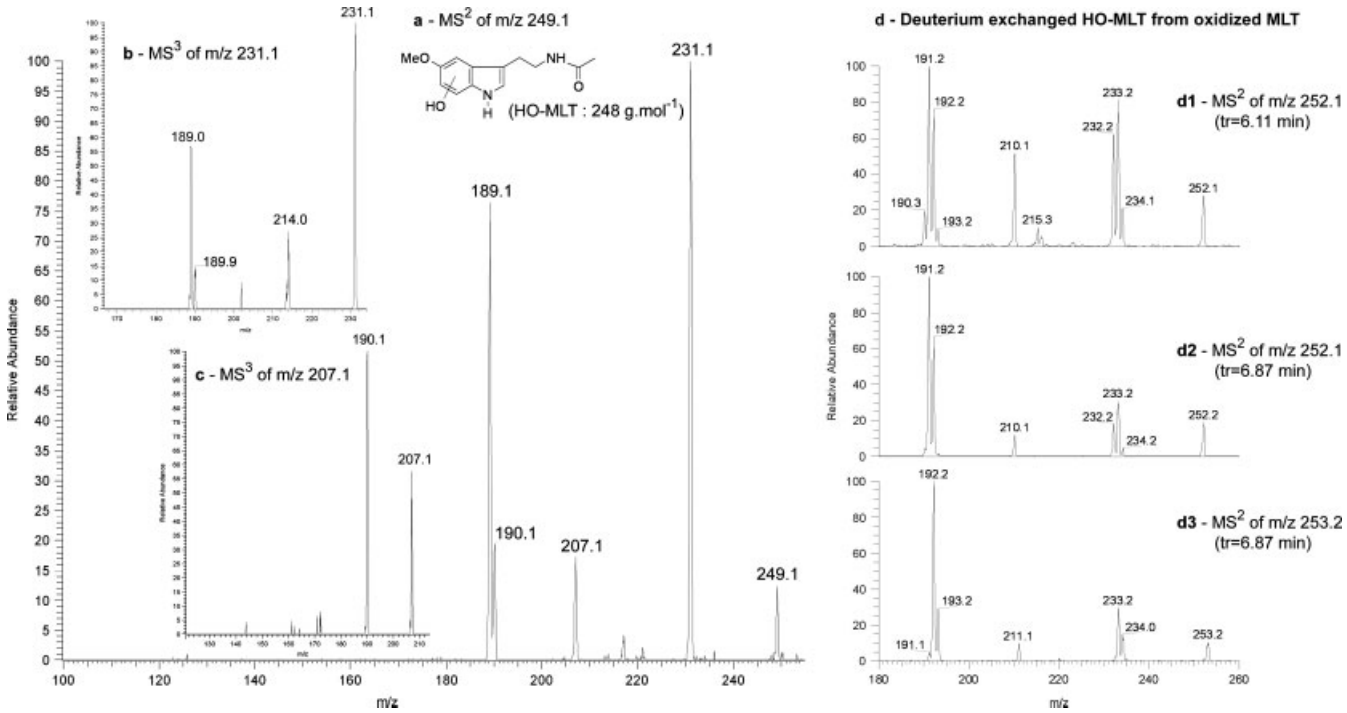

Figure 5. (a) CID spectrum of the ion at *m/z* 249.1 for an aerated aqueous solution of MLT (100 µmol l^{-1}), irradiated at 340 Gy; (b) MS^3 spectrum of the product ion at *m/z* 231.1; (c) MS^3 spectrum of the product ion at *m/z* 207.1; (d) CID spectrum of the ion at *m/z* 252.1 (*m/z* 249 + 3 deuterium exchanges) for the chromatographic peaks detected at t_r = 6.11 min (d1) and t_r = 6.87 min (d2), and CID spectrum of the ion at *m/z* 253.2 (*m/z* 249 + 4 deuterium exchanges) for the chromatographic peak detected at t_r = 6.87 min (d3): retention time refers to the chromatogram obtained for HPLC working with deuterated eluent (Fig. 3).

the possibility of a double proton exchange during fragmentation. In addition, detection of four peaks at *m/z* 190.3, 191.2, 192.2 and 193.2 essentially implies the same phenomenon. For the second product (t_r = 6.87, Fig. 5 (d2) and (d3)), H/D scrambling occurs via a different pathway; only two peaks are detected at *m/z* 191.2 and *m/z* 192.2, along with two main peaks at *m/z* 232.2 and 233.2, for the fragmentation of *m/z* 252.2 (Fig. 5 (d2)). This shows that H/D scrambling does not occur as previously observed for the first product. The CID spectrum of fully deuterated xHO-MLT (Fig. 5 (d3)) supports this assumption.

Scheme 3 proposes a general fragmentation pathway for deuterated xHO-MLT. The first pathway of *m/z* 253 fragmentation

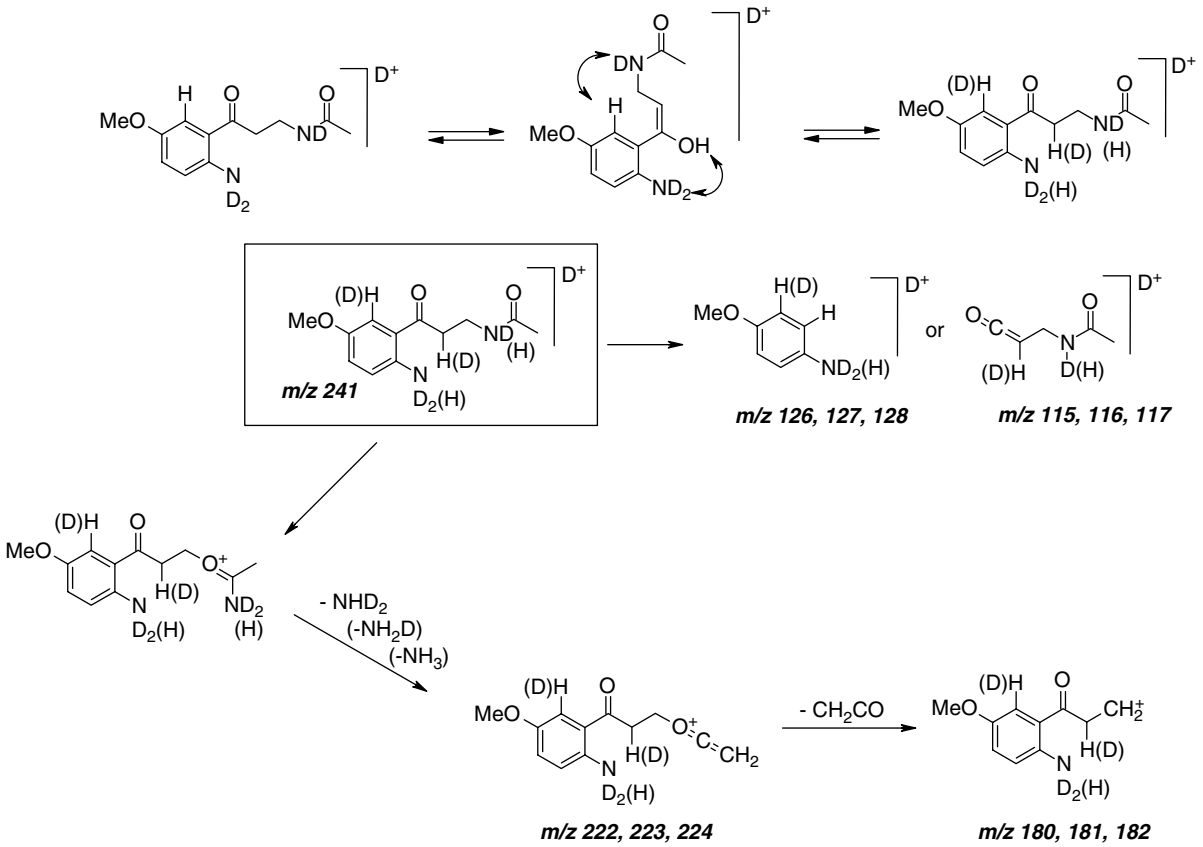

Scheme 2. The proposed H/D scrambling and fragmentation pathway for deuterated AMK.

(Scheme 3(a)), where both protons of the indole ring are susceptible to exchange, involves the loss of variably deuterated water, followed by the fixed loss of CH_2CO; this leads to three peaks at *m/z* 233, 234, 235 and three at *m/z* 191, 192, 193. The transition *m/z* 211 → *m/z* 194 results from a loss of non-deuterated ammonia from the *N*-acetyl group implying a double proton exchange during H/D scrambling. This first fragmentation pathway, involving the highest multiplicity of product ions, seems to be the pathway observed for the first product. A second pathway is proposed in Scheme 3(b), for 2HO- and 4HO-MLT in which only one proton of the indole ring can exchange during fragmentation. The blocking of one exchangeable position logically leads to the loss of HDO and D_2O (*m/z* 253 → *m/z* 234, 233), and NH_2D and NHD_2 (*m/z* 253 → *m/z* 211 → *m/z* 192, 193). The multiplicity of the product ions is lower than the previous one, and this pathway is in good agreement with the CID spectrum of the second product. Finally, the oxidation products at *m/z* 249 probably correspond to 6HO- or 7HO-MLT on the one hand, and 2HO- or 4HO-MLT on the other.

Identification of the products detected at *m/z* 263 and *m/z* 265

As mentioned, AFMK is known to result from the oxidation of MLT *in vivo*. AFMK has a molecular weight of 264 g mol^{-1} and thus could be a good candidate in the identification of the oxidation product detected at *m/z* 265. To test this assumption, AFMK was synthesised and CID mass spectra (for AFMK 50 µmol l^{-1}) were obtained for the precursor ion at *m/z* 265 and product ions at *m/z* 237 and *m/z* 247 (Fig. 6(a)), and compared with those of similar ions in an aerated aqueous solution of MLT (100 µmol l^{-1}) irradiated at 200 Gy (Fig. 6(b)). Fragmentation of synthetic AFMK leads to two product ions at *m/z* 246.9 and *m/z* 236.9 (losses of −18 and −28 Da, respectively). Fragmentation of this last ion generates second-generation ions at *m/z* 219.7, *m/z* 177.9 and *m/z* 114.0 (losses of −17, −59 and −123 Da, inset of Fig. 6(a)). The similar MS/MS and MS^3 CID spectra are observed for the ion at *m/z* 265.0 from a solution of oxidised MLT (Fig. 6(b) and inset, respectively). These results suggest that AFMK is one of the oxidation products of MLT in our experimental conditions.

As AFMK is based on the same chemical structure as AMK (structures given in Figs 4 and 6), some similarities should be observed for their fragmentation pathways. This is verified, in particular for the product ion at *m/z* 237: the CID spectrum of this ion for synthetic AMK (Fig. 4) is very close to the one observed for AFMK (Fig. 6), even in the deuterated medium D_2O/MeOD (Fig. 7(a), inset). First, this suggests that the product ion of AFMK at *m/z* 237 has the same structure as AMK. In addition, H/D scrambling could proceed by the same route as proposed in Scheme 4. After the loss of a 28 Da (CO), the product ion at *m/z* 240 (in labelled medium) follows the same fragmentation pathway as AMK and leads to two series of three consecutive peaks at *m/z* 179.0, 180.1, 181.0 and *m/z* 114.0, 114.9, 116.0 (Fig. 7(a), inset). The second pathway (Scheme 4) for AFMK fragmentation generates product ions at *m/z* 248, 249, 250 by the loss of variably deuterated water or ammonia; loss of CH_2CO then leads to the peaks at *m/z* 206, 207, 208. The fragmentation pathway proposed in Scheme 4 is in good agreement with the experimental CID spectra of AMK and AFMK. The CID spectrum of deuterated AFMK from oxidised MLT (Fig. 7(b)) contains product ions at *m/z* 248, 249, 250, *m/z* 239, 240,

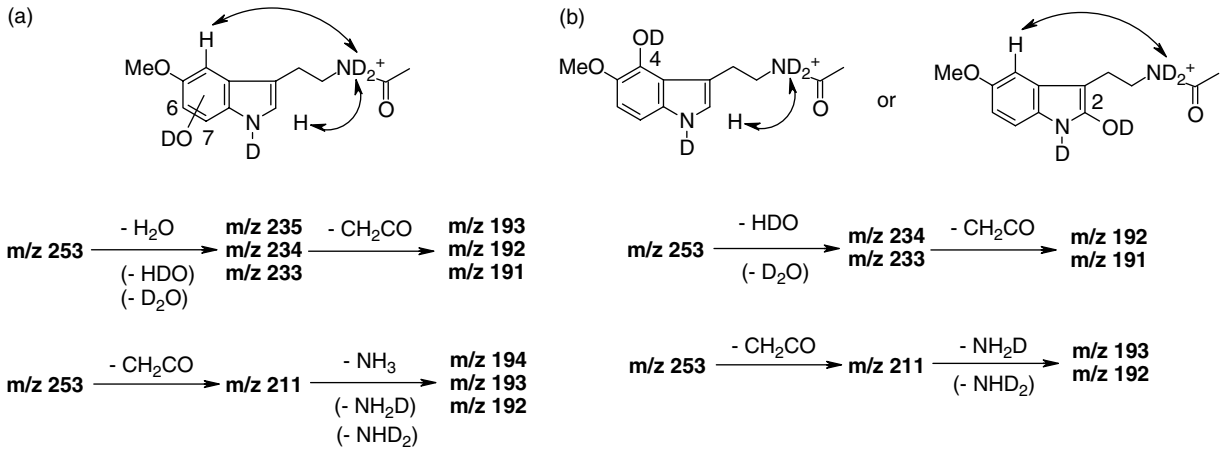

Scheme 3. The proposed H/D scrambling and general fragmentation scheme for deuterated (a) 6HO- or 7HO-MLT and (b) 2HO- or 4HO-MLT.

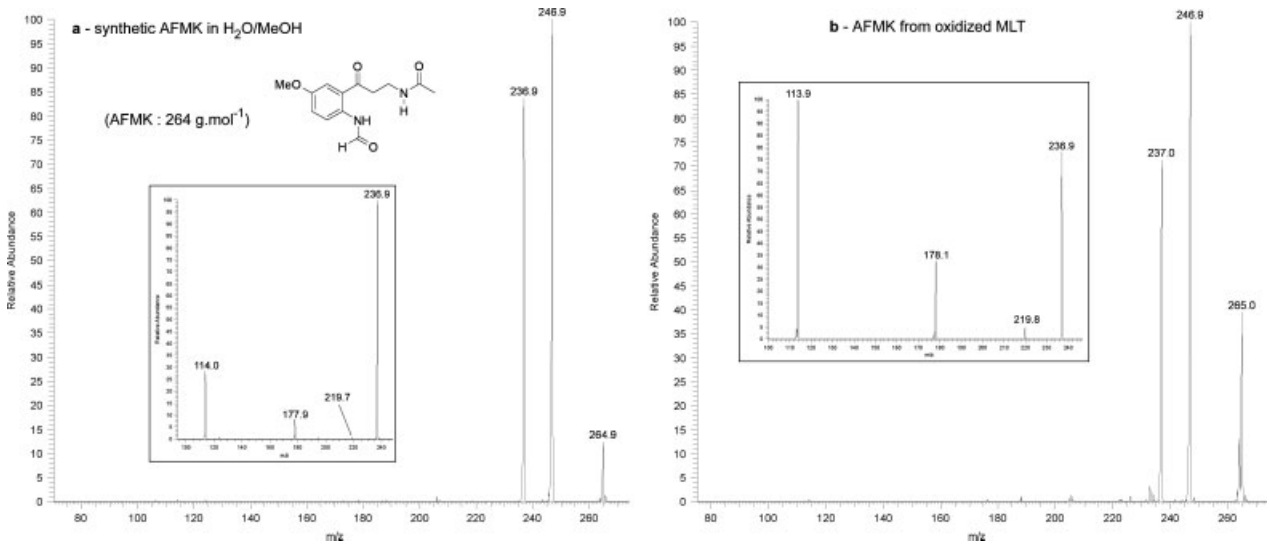

Figure 6. (a) CID spectrum of the ion at *m/z* 264.9 for a solution of synthetic AFMK (50 µmol l^{-1}) in H_2O/MeOH (1/10 v/v); inset: MS^3 spectrum of the product ion at *m/z* 236.9, (b) CID spectrum of the ion at *m/z* 265.0 for an aerated aqueous solution of MLT (100 µmol l^{-1}), irradiated at 200 Gy; inset: MS^3 spectrum of the product ion at *m/z* 236.9.

m/z 179, 180, 181 and *m/z* 115, 116 as observed for deuterated synthetic AFMK. In addition, the loss of CH_2CO leads to the product ion at *m/z* 226, whose fragmentation generates multiple peaks at *m/z* 206, 207, 208 by the loss of variably deuterated water or ammonia. These results provide an additional confirmation that the irradiated solution of MLT contains AFMK as one of the oxidation products.

The last oxidation product was detected at *m/z* 263.1 and $t_r = 4.53$ min (Fig. 3). On the basis of its mass and by comparison with those of the other oxidation products, we suggest that *m/z* 263 could result from a dehydrogenation of AFMK (dehydro-AFMK or dH-AFMK).

MS/MS and MS^3 spectra of the ion detected at *m/z* 263.2 for an aerated aqueous solution of MLT (200 µmol l^{-1}) irradiated at 440 Gy are presented in Fig. 8(a) together with the proposed structure of dH-AFMK, which contains a conjugated double bond on the aliphatic chain. Because of the similarity in chemical structures between dH-AFMK on the one hand and AMK and AFMK on the other, similar losses are expected during the fragmentation process. Indeed, fragmentation of *m/z* 263.2 shows successive losses of −42 Da (263.2 → 221.1) and −17 Da (221.1 → 204.1) by one pathway, and −18 Da (263.2 → 245.1) and −42 Da (245.1 → 203.2) by the second pathway (Fig. 8(a)). All these losses have been previously observed in AMK and AFMK fragmentation (Figs 4 and 6, respectively); they correspond to the loss of CH_2CO, NH_3 or H_2O. In addition, the CID spectrum of the product ion at *m/z* 245.4 (Fig. 8, inset right) exhibits a peak at *m/z* 132.9, resulting from a loss of −112 Da that could correspond to the whole aliphatic chain of dH-AFMK (CH_3–CO–NH–CH=CH–CO) and thus confirms the proposed position of the double bond. These experimental results strongly suggest that dH-AFMK is an oxidation product of MLT in our experimental conditions.

The CID spectrum of the product detected at $t_r = 5.65$ min during chromatographic separation of oxidised MLT with deuterated eluent (Fig. 8(b)) is in good agreement with the chemical structure of dH-AFMK (precursor ion at *m/z* 266.1 = 263.2 + 3 deuterium exchanges). The main product ion is detected as a single peak at *m/z* 224.1 (= 221.1 + 3) and corresponds to the loss of CH_2CO. As proposed in Scheme 4, the losses of either CH_2CO or variably deuterated water or ammonia lead first to product ions at *m/z*

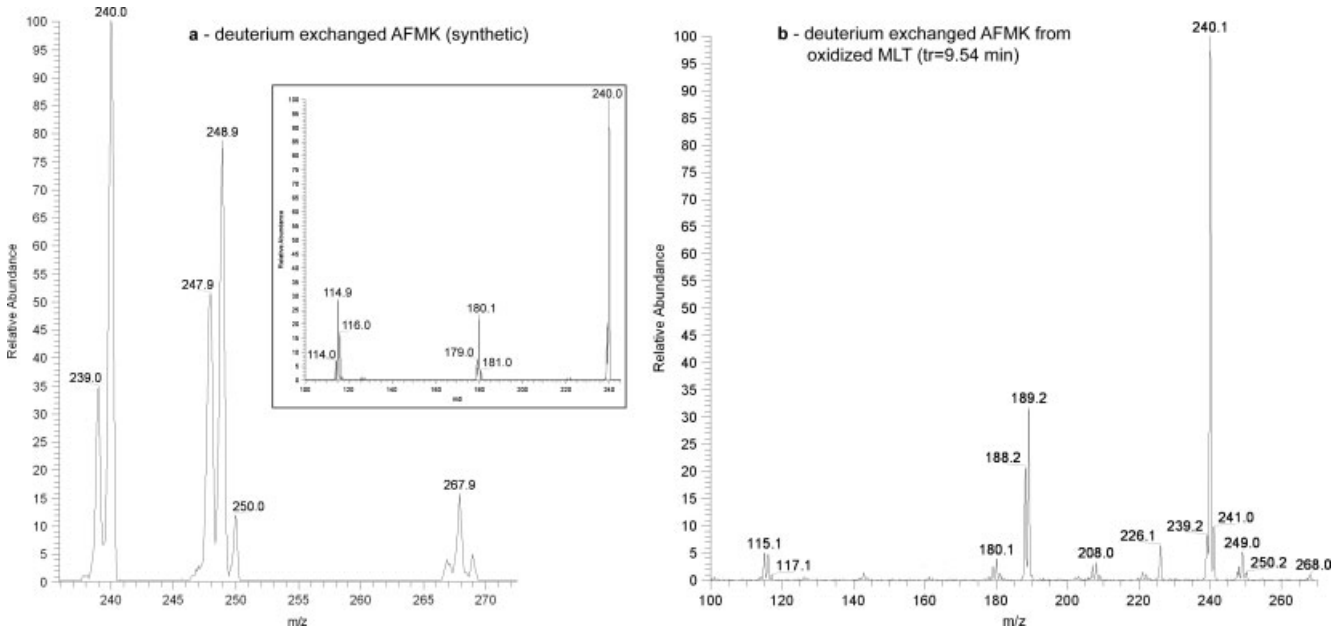

Figure 7. CID spectrum of the ion at *m/z* 267.9 (AFMK + 3 deuterium exchanges) for a solution of synthetic AFMK (50 µmol l^{-1}) in D_2O/MeOD (1/1 v/v); inset: MS^3 spectrum of the product ion at *m/z* 240.0, (b) CID spectrum of the ion at *m/z* 268.0 (*m/z* 265 + 3 deuterium exchanges) for the chromatographic peak detected at t_r = 9.54 min; retention time refers to the chromatogram obtained for HPLC working with deuterated eluent (Fig. 3).

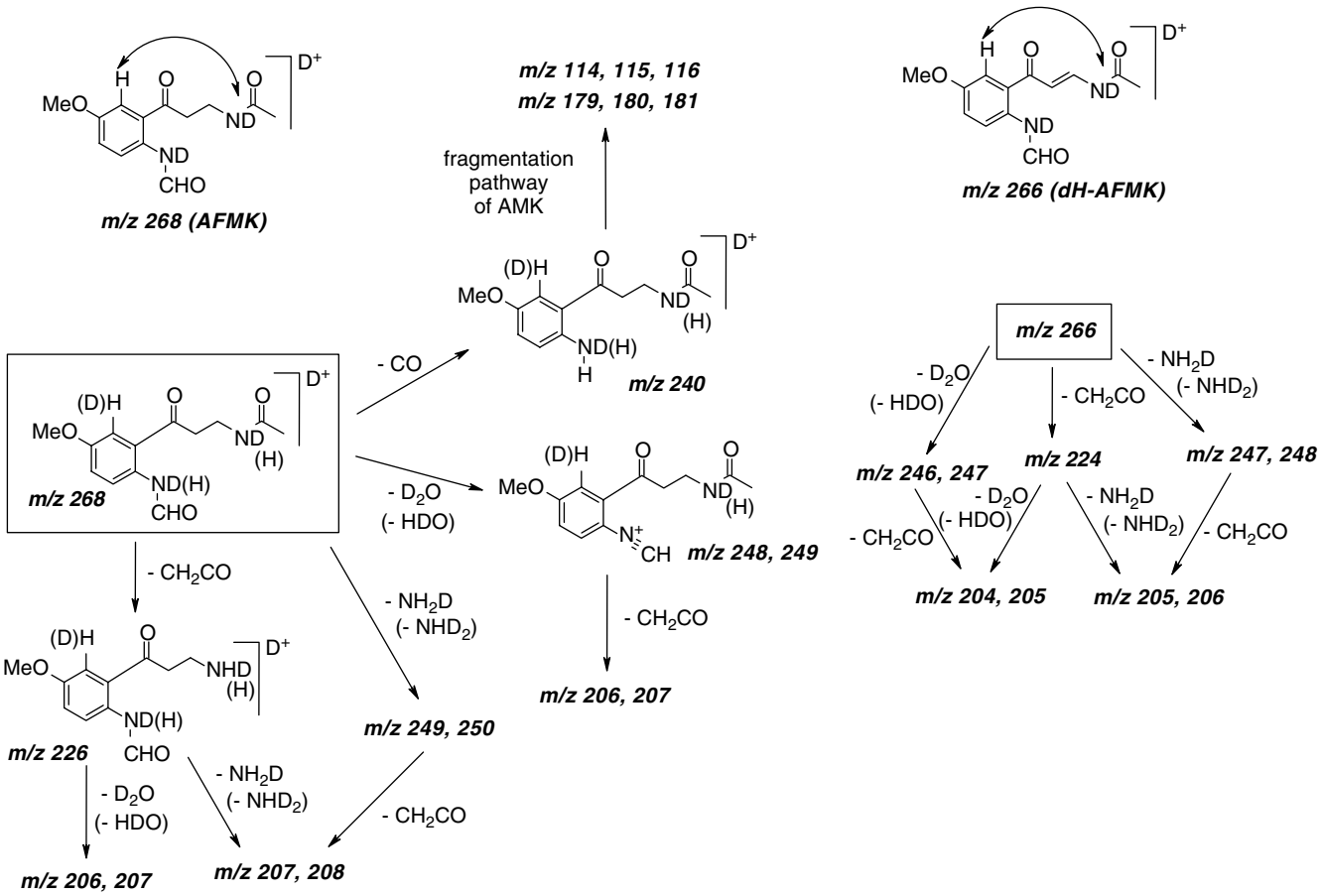

Scheme 4. The proposed H/D scrambling and fragmentation pathway for deuterated AFMK and dH-AFMK.

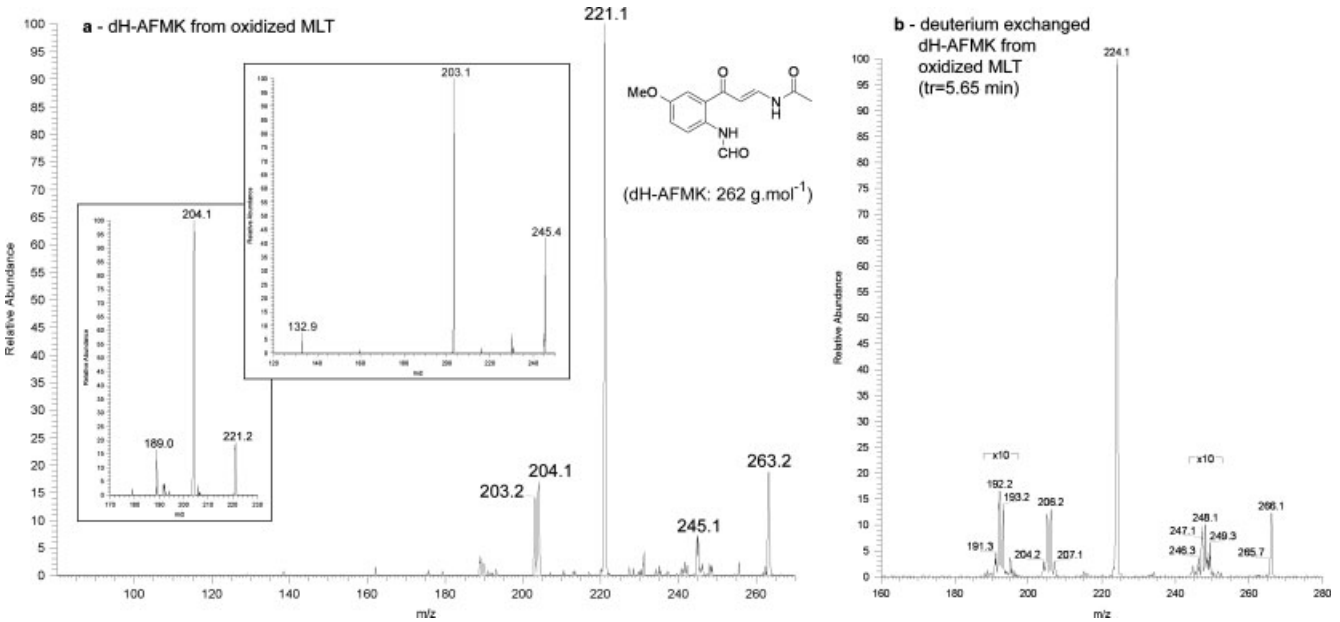

Figure 8. CID spectrum of the ion at *m/z* 263.2 for a solution of MLT (200 μmol l^{-1}) irradiated at 440 Gy; insets: MS^3 spectra of product ions at *m/z* 245.4 (right) and *m/z* 221.2 (left); (b) CID spectrum of the ion at *m/z* 266.2 (*m/z* 263 + 3 deuterium exchanges) for the chromatographic peak detected at $t_r = 5.65$ min: retention time refers to the chromatogram obtained for HPLC working with deuterated eluent (Fig. 3).

224 and 246, 247, 248, and then to second-generation ions at *m/z* 204, 205, 206. This pathway is in good agreement with the experimental CID spectrum shown in Fig. 8(b). The study of H/D scrambling confirms that dH-AFMK is detected in aqueous solution of oxidised MLT.

Conclusion

MLT was oxidised by hydroxyl free radicals, the most reactive species involved in oxidative stress phenomena *in vivo*. MLT acts as an antioxidant towards hydroxyl radicals and its oxidation leads to several end-products. As a tryptophan-related compound, deuterated MLT shows a similar behaviour regarding H/D scrambling during the gas-phase fragmentation process. This leads to specific CID spectra of MLT and its oxidation end-products, and was used for identification; thus, AMK, AFMK, dH-AFMK and HO-MLT were identified as oxidation end-products of MLT *in vitro* in our conditions. For each product, experimental CID spectra and studies of H/D exchange established fragmentation pathways in good agreement with chemical structures: AMK and AFMK on the one hand, and MLT and HO-MLT on the other, show similarity in the losses and H/D scrambling. In particular, *N*-acetyl deuterium may exchange with protons in the C2 and C4 positions of the indole ring and thus leads to variable losses during fragmentation. The characteristic H/D scrambling of MLT and its oxidation products during MS fragmentation, coupled with liquid chromatography in labelled eluent, allowed the identification of two hydroxylated isomers of MLT: 2HO- or 4HO-MLT, and 6HO- or 7HO-MLT. The same type of H/D scrambling was postulated for AMK, AFMK and dH-AFMK in which *N*-acetyl deuterium exchanges with proton on the benzene ring. Studies on the particular deuterium exchange behaviour of MLT and related compounds give reliable information for characterisation.

Furthermore, this work shows that we anticipate relatively few differences regarding the nature of products formed under our *in vitro* conditions and under those of catabolism, since the oxidation products identified *in vitro* in our experimental conditions have already been identified *in vivo* as mentioned previously. Water radiolysis thus seems to be well adapted to mimic an oxidative stress condition.

References

[1] R. Hardeland. Antioxidative protection by melatonin. *Endocrine* **2005**, *27*, 119.
[2] D. X. Tan, R. J. Reiter, L. C. Manchester, M. T. Yan, M. El Sawi, R. M. Sainz, J. C. Mayo, R. Kohen, M. Allegra, R. Hardeland. Chemical and physical properties and potential mechanisms: melatonin as a broad spectrum antioxidant and free radical scavenger. *Current Topics in Medicinal Chemistry* **2002**, *2*, 181.
[3] I. Gulcin, M. E. Buyukokuroglu, M. Oktay, O. I. Kufrevioglu. On the *in vitro* antioxidative properties of melatonin. *Journal of Pineal Research* **2002**, *33*, 167.
[4] Vijayalaxmi, R. J. Reiter, M. L. Meltz. Melatonin protects human blood lymphocytes from radiation induced chromosome damage. *Mutation Research* **1995**, *34*, 623.
[5] M. A. El-Missiry, T. A. Fayed, M. R. El-Sawy, A. A. El-Sayed. Ameliorative effect of melatonin against gamma-irradiation-induced oxidative stress and tissue injury. *Ecotoxicology and Environmental Safety* **2007**, *66*, 278.
[6] H. Kaya, B. Oral, F. Ozguner, V. Tahan, Y. Babar, N. Delibas. The effect of melatonin application on lipid peroxidation during cyclophosphamide therapy in female rats. *Zentralblatt Fur Gynakologie* **1999**, *12*, 499.
[7] Viajayalaxmi, R. J. Reiter, T. S. Herman, M. L. Meltz. Melatonin and radioprotection from genetic damage: *in vivo/in vitro* studies with human volunteers. *Mutation Research* **1996**, *37*, 221.
[8] Viajayalaxmi, R. J. Reiter, M. L. Meltz. Melatonin: possible mechanisms involved in its "radioprotective" effect. *Mutation Research* **1998**, *404*, 187.
[9] Z. Matuszak, K. J. Reszka, C. F. Chignell. Reaction of melatonin and related indoles with hydroxyl radicals: EPR and spin trapping investigations. *Free Radical Biology and Medicine* **1997**, *23*, 367.
[10] B. Poeggeler, S. Thuermann, A. Dose, M. Schoenke, S. Burkhardt, R. Haderland. Melatonin's unique radical scavenging properties-

roles of its functional substituents as revealed by a comparison with its structural analogs. *Journal of Pineal Research* **2002**, *33*, 20.
[11] J. E. Roberts, D. H. Hu, J. F. Wishart. Pulse radiolysis studies of melatonin and chloromelatonin. *Journal of Photochemistry and Photobiology B-Biology* **1998**, *42*, 125.
[12] M. A. Livrea, L. Tesoriere, D. D'Arpa, M. Morreale. Reaction of melatonin with lipoperoxyl radicals in phospholipid bilayers. *Free Radical Biology and Medicine* **1997**, *23*, 706.
[13] C. Pieri, M. Marra, F. Moroni, R. Recchioni, F. Marcheselli. Melatonin: A peroxyl radical scavenger more effective than vitamin E. *Life Sciences* **1994**, *55*, PL271.
[14] E. Walters-Laporte, C. Furman, S. Fouquet, F. Martin-Nizard, S. Lestavel, A. Gozzo, D. Lesieur, J. C. Fruchart, P. Duriez, E. Teissier. A high concentration of melatonin inhibits *in vitro* LDL peroxidation but not oxidized LDL toxicity toward cultured endothelial cells. *Journal of Cardiovascular Pharmacology* **1998**, *32*, 582.
[15] L. Y. Zang, G. Cosma, H. Gardner, V. Vallyathan. Scavenging of reactive oxygen species by melatonin. *Biochimica Et Biophysica Acta* **1998**, *1425*, 469.
[16] P. H. Abuja, P. Liebmann, M. Hayn, K. Schauenstein, H. Esterbauer. Antioxidant role of melatonin in lipid peroxidation of human LDL. *FEBS Letters* **1997**, *413*, 289.
[17] D. Bonnefont-Rousselot, G. Cheve, A. Gozzo, A. Tailleux, V. Guilloz, S. Caisey, E. Teissier, J. C. Fruchart, J. Delattre, D. Jore, D. Lesieur, P. Duriez, M. Gardès-Albert. Melatonin related compounds inhibit lipid peroxidation during copper or free radical-induced LDL oxidation. *Journal of Pineal Research* **2002**, *33*, 109.
[18] M. Allegra, R. J. Reiter, D. X. Tan, C. Gentile, L. Tesoriere, M. A. Livrea. The chemistry of the melatonin's interaction with reactive species. *Journal of Pineal Research* **2003**, *34*, 1.
[19] S. R. Schaffazick, A. R. Pohlmann, C. A. S. de Cordora, T. B. Creczynski-Pasa, S. S. Guterres. Protective properties of melatonine-leaded nanoparticles against lipid peroxidation. *International Journal of Pharmaceutics* **2005**, *289*, 209.
[20] D. X. Tan, L. C. Manchester, R. J. Reiter, B. F. Plummer, L. J. Hardies, S. T. Weintraub, Vijayalaxmi, A. M. M. Shepard. A novel melatonin metabolite, cyclic 3-hydroxymelatonin: A biomarker of in vivo hydroxyl radical generation. *Biochemical and Biophysical Research Communications* **1998**, *253*, 614.
[21.] J. W. T. Spinks, R. J. Woods. Water and inorganic aqueous systems. *Introduction to Radiation Chemistry*, 3rd edn. (A Wiley Interscience publication) Wiley: New York, **1990**, 243.
[22] H. S. Mahal, H. S. Sharma, T. Mukherjee. Antioxidant properties of melatonin: a pulse radiolysis study. *Free Radical Biology and Medicine* **1999**, *26*, 557.
[23] H. Fricke, S. Morse. The chemical action of Roentgen rays on dilute ferrosulfonate solutions as a measure of dose. *American Journal of Roentgenology Radium Therapy and Nuclear Medicine* **1927**, *18*, 430.
[24] E. A. Almeida, C. F. Klitzke, G. R. Martinez, M. H. G. Medeiros, P. Di Mascio. Synthesis of internal labelled standards of melatonin and its metabolite N1-acetyl-N5 methoxykynurenine for their quantification using an on-line liquid chromatography-electrospray tandem mass spectrometry system. *Journal of Pineal Research* **2004**, *36*, 64.
[25] G. Diamantini, G. Tarzia, G. Spadoni, M. D'Alpaos, P. Traldi. Metastable ion studies in the characterization of melatonin isomers. *Rapid Communications in Mass Spectrometry* **1998**, *12*, 1538.
[26] H. Lioe, R. A. J. O'Hair, G. E. Reid. Gas-phase reactions of tryptophan. *Journal of the American Society for Mass Spectrometry* **2004**, *15*, 65.
[27] S. Steenken. Addition-elimination paths in electron-transfer reactions between radicals and molecules. *Journal of the Chemical Society-Faraday Transactions* **1987**, *83*, 113.
[28] C. Harthe, D. Claudy, H. Dechaud, B. Vivien-Roels, P. Pevet, B. Claustrat. Radioimmunoassay of N-acetyl-N-formyl-5-methoxykynuramine (AFMK): a melatonin oxidative metabolite. *Life Sciences* **2003**, *73*, 1587.
[29] R. J. Reiter, D. X. Tan, C. Osuna, E. Gitto. Actions of melatonin in the reduction of oxidative stress: A review. *Journal of Biomedical Science* **2000**, *7*, 444.
[30] S. O. Silva, M. R. Rodrigues, S. R. Q. Carvalho, L. H. Catalani, A. Campa, V. F. Ximenes. Oxidation of melatonin and its catabolites, N^1-acetyl-N^2-formyl-5-methoxykynuramine and N^1-acetyl-5-methoxykynuramine, by activated leukocytes. *Journal of Pineal Research* **2004**, *37*, 171.
[31] S. Bourcier, J.-F. Benoist, F. Clerc, O. Rigal, M. Taghi, Y. Hopilliard. Detection of 28 neurotransmitters and related compounds in biological fluids by liquid chromatography/tandem mass spectrometry. *Rapid Communications in Mass Spectrometry* **2006**, *20*, 1405.
[32] D. X. Tan, L. C. Manchester, M. P. Terron, L. J. Flores, R. J. Reiter. One molecule, many derivatives: A never-ending interaction of melatonin with reactive oxygen and nitrogen species? *Journal of Pineal Research* **2007**, *42*, 28.
[33] P. Stasica, P. Paneth, J. M. Rosiak. Hydroxyl radical reaction with melatonin molecule: a computational study. *Journal of Pineal Research* **2000**, *29*, 125.

